NASA Technical Memorandum 82927

Extending the Frequency of Response of Lightly Damped Second Order Systems: Application to the Drag Force Anemometer

Gustave C. Fralick
Lewis Research Center
Cleveland, Ohio

August 1982

NASA

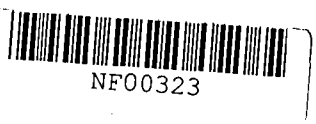

EXTENDING THE FREQUENCY OF RESPONSE OF LIGHTLY DAMPED SECOND ORDER SYSTEMS: APPLICATION TO THE DRAG FORCE ANEMOMETER

Gustave C. Fralick

National Aeronautics and Space Administration
Lewis Research Center
Cleveland, Ohio 44135

E-1178

SUMMARY

It is shown in this paper that a conventional electronic frequency compensator does not provide adequate compensation near the resonant frequency of a lightly damped second order system, such as the drag force anemometer. The reason for this is discussed, and a simple circuit modification is presented which overcomes the difficulty. The improvement is shown in theoretical frequency response curves as well as in the experimental results from some typical drag force anemometers.

INTRODUCTION

The use of electrical or electronic means to extend the frequency response of a transducer is not new. For instance, passive electrical networks have long been used to improve the response of thermocouples (ref. 1), and a frequency compensation is a practical necessity in hot wire anemometry, raising the useful frequency range from a few hundred Hz to nearly 100 kHz.

A similar situation has arisen in the application of the drag force anemometer (ref. 2), which is a probe that is used to measure either velocity head or flow angle in moving fluids. Because of the design of the device, which is described in greater detail in the next section, it has inherently 2ood frequency response. Some designs have a natural frequency as high as 43 kHz, but there arise situations such as flow monitoring in jet engines, where frequencies as high as 100 kHz are of interest. This paper describes the problems encountered in applying a frequency compensator to the drag force anemometer, describes the remedy, and describes the results of using a modified compensator on sample drag force anemometers.

By way of background, the paper begins with a brief description of the drag force anemometer and then a brief discussion of second order systems in general. Next, electronic frequency compensation is discussed along with the problems encountered in applying compensation to the drag force anemometer. It is then shown that the problem may be overcome by means of a simple change in the compensator circuit. Both calculated and experimental results are presented which show the improvement. The detailed mathematics are given in an appendix.

DESCRIPTION OF THE DRAG FORCE ANEMOMETER

The drag force anemometer has found application in many different flow measurement areas. Some of the applications are described in reference 2.

The drag force anemometer is a cantilever beam, with strain gauges mounted near the base. When the free end of the beam is exposed to a moving fluid, the fluid exerts a drag force $F(t)$ on the beam. If the beam orientation is approximately normal to the flow, $F(t)$ is proportional to the velocity head of the moving fluid. If the beam is oriented so that the flow is roughly parallel to the beam, $F(t)$ is proportional to the product of the velocity head and flow angle (see figure 1). Thus, in one probe, one has a tool for measuring both velocity head and flow angle.

The drag force exerted by the fluid on the beam causes a strain in the beam and a resistance change in the strain gauges. This is turned into an electrical signal $\chi(t)$ by the associated electronics.

It is shown in reference 2 that the dynamic response of the anemometer is described by the equation.

$$\ddot{\chi}/\omega_n^2 + 2\zeta\,\dot{\chi}/\omega_n + \chi = \kappa\,F(t) \qquad (1)$$

The parameter $f_n = \omega_n/2\pi$ is the natural frequency, ζ is the damping coefficient, and κ is a proportionality constant.

If f_n is large compared to any frequency in the flow, the first two terms in equation (1) may be omitted, and equation (1) reduces to $\chi = \kappa F(t)$; that is, $\chi(t)$ is directly proportional to $F(t)$ and the output is an accurate representation of the dynamic velocity head (or product of velocity head and flow angle, as explained above). Hence, one way to improve the frequency response is to increase the natural frequency. The natural frequency can be increased by making the beam of a high specific stiffness material such as silicon or alumina, instead of a material like stainless steel, whose specific stiffness is lower. The natural frequency can also be increased by making the beam shorter and thicker, but this reduces sensitivity.

The drag force anemometer shown in figure 2 has a beam made of silicon and a natural frequency of 42.8 kHz. This is the highest natural frequency of any of the beams built at the Lewis Research Center.

DYNAMIC BEHAVIOR OF SECOND ORDER SYSTEMS

The frequency response of the drag force anemometer and other second order systems (i.e., systems described by linear second order differential equations such as eq. (1)) may be examined by letting the driving function $\kappa F(t) = \mathscr{E}_0 \sin \omega t$, with $\mathscr{E}_0$ constant. With this function on the right side of equation (1), the solution $\chi(t)$ is

$$\chi(t) = A \sin \omega t + B \cos \omega t = R(\omega) \sin [\omega t - \varphi(\omega)]$$

$$R(\omega) = \sqrt{A^2 + B^2}\,, \quad \tan [\varphi(\omega)] = B/A$$

$$
\left.
\begin{aligned}
A(\omega) &= \mathscr{E}_0 \left(1 - \frac{\omega^2}{\omega_n^2}\right) \Big/ \Delta \\
B(\omega) &= -2\,\mathscr{E}_0\,\zeta\omega/\omega_n\Delta \\
\Delta &= \left(1 - \frac{\omega^2}{\omega_n^2}\right)^2 + 4\,\zeta^2\,\frac{\omega^2}{\omega_n^2}
\end{aligned}
\right\} \qquad (2)
$$

The amplitude R and phase shift φ are

$$
\left.
\begin{aligned}
R(\omega) &= \mathscr{E}_0 \sqrt{\left(1 - \frac{\omega^2}{\omega_n^2}\right)^2 + 4\,\zeta^2\,\frac{\omega^2}{\omega_n^2}} \\
\varphi(\omega) &= \tan^{-1}\left[2\,\zeta\,\frac{\omega}{\omega_n} \Big/ \left(1 - \frac{\omega^2}{\omega_n^2}\right)\right]
\end{aligned}
\right\} \qquad (3)
$$

The amplitude response defined as $20 \log R/\mathscr{E}_0$ and φ are plotted in figures 3 and 4 for the case $f_n = 1300$ Hz and $\zeta = 0.024$. These values are for a drag force anemometer similar to the one in figure 2, except that the beam is slightly longer and made of stainless steel rather than silicon.

The figures for different damping coefficients would be essentially the same, with the peak near f_n being higher and sharper for smaller values of ζ; such figures are widely available throughout the technical literature.

These figures show that the amplitude response and φ are strongly dependent on frequency above $f/f_n \approx 0.2$. In fact, for this example, the amplitude increase is about 4 percent (0.4 dB) at $f = 0.2\,f_n$ and is about 10 percent (0.8 dB) at $f = 0.3\,f_n$. If no correction is made, these changes become measurement errors, in addition to any other system errors present. They are an inherent characteristic of second order systems.

Even if higher frequencies are not of interest in the measurement, there may be frequency components in the flow that can excite a drag force anemometer beam to resonance. The result is a signal in which the low frequency information is obscured by large amplitude oscillations at the natural frequency.

COMPENSATION: PRINCIPLES OF OPERATION

Since the problem with using the drag force anemometer to make dynamic flow measurements is that the amplitude response and phase vary with frequency, a solution would be to feed the signal into a device (amplifier) whose gain and phase shift varied with frequency in a manner exactly the inverse of the way they vary in the anemometer. The large increase in amplitude response near the natural frequency would be attenuated, but for higher

frequencies the gain would increase, making up for the decreasing sensitivity of the anemometer.

This is what happens in the compensator, but instead of viewing it as a device whose gain varies with frequency, it is easier to understand the principle of operation by considering what it does to the signal it gets from the anemometer. As is shown in figure 5, the anemometer output $\chi(t)$ is fed into the compensator which electronically performs on $\chi(t)$ all of the mathematical operations indicated in equation (1). The ideal differentiators introduce a phase shift of 90° at the output of the first differentiator and a phase shift of 180° at the output of the second differentiator, both referred to the input. This compensation completely eliminates the peak centered at $f = f_n$ shown in figure 3. The output is $\kappa F(t)$, which is the desired signal. This topic is discussed more fully in reference 3.

COMPENSATION: SOME PRACTICAL CONSIDERATIONS

Since real circuits and real signals are not ideal but always have noise associated with them, some practical considerations arise in the application of compensators. One consideration is that it is not possible to extend the frequency range indefinitely. As the sensitivity of the anemometer continues to drop, a point will be reached where the signal from the anemometer will be buried in the noise at that frequency and the compensator will not distinguish between them. Another consideration is that because of the differentiators it contains, a compensator tends to act as a noise source in its own right. As is explained in reference 4, the gain of a differentiator increases linearly with frequency, so it amplifies any high-frequency noise.

A standard operational amplifier differentiator circuit is shown in figure 6(a). In order to reduce the noise, the circuit must be modified so that the gain does not continue to increase with frequency. The usual modification is to add a small resistor in series with the input capacitor, and to add a small feedback capacitor. The modified circuit is shown in figure 6(b). These changes reduce the gain at high frequencies, but permit approximate differentiation at lower frequencies. All the compensators discussed in this report, whether called "conventional" or "modified", are assumed to be built with modified differentiators.

A compensator built using the modified differentiators shown in figure 6(b) had a peak-to-peak noise of about 5 mV (0 to 100 kHz) with the input shorted. This is acceptable in most applications of the drag force anemometer.

ADDITIONAL CONSIDERATIONS FOR SYSTEMS WITH LOW DAMPING

Because of the modifications required in the differentiators, their output is no longer exactly proportional to the derivative of the input; there is now a small error. When these modified differentiators are incorporated into a compensator, there is also an overall compensator error. The error is most important for frequencies near f_n, and the size of the error is related to the size of the damping coefficient.

The example plotted in figure 7 shows that if the damping coefficient is not too small, the conventional compensator of figure 5 is able to achieve adequate compensation by maintaining the amplitude response flat to within 1 dB for frequencies out to about two and one-half times f_n. Note that unlike the results obtained with perfect differentiators, the peak is not completely eliminated since cancellation occurs only at f_n and not over

the entire frequency range. Figure 8, however, shows that for a system with a smaller damping coefficient the conventional circuit (with modified differentiators) is unable to provide adequate compensation due primarily to an inability to achieve cancellation at $f = f_n$.

Fortunately, it turns out that just by removing the inverter from the circuit of figure 5, the cancellation at f_n can be restored. The details are in appendix B, but the idea can be discussed briefly here.

To see what causes the problem, suppose that the compensator input is $e_1 = \mathscr{A} \sin \omega t$. Let the output of the first differentiator be e_2 and the output of the second be e_3, and let the damping adjustment be set at $2k$.

With a compensator input $e_1 = \mathscr{A} \sin \omega t$, equation (B10) of appendix B gives for e_2

$$e_2 \simeq -\mathscr{A} \frac{\omega}{\omega_n} \cos (\omega t - \theta) = \mathscr{A} \frac{\omega}{\omega_n} \sin \left[\omega t - \left(\frac{\pi}{2} + \theta \right) \right] \tag{4}$$

and equation (B11) of appendix B gives for e_3

$$e_3 \simeq -\mathscr{A} \frac{\omega^2}{\omega_n^2} \sin (\omega t - 2\theta) = \mathscr{A} \frac{\omega^2}{\omega_n^2} \sin [\omega t - (\pi + 2\theta)] \tag{5}$$

A perfect differentiator introduces a phase shift of $\pi/2$ between its input and output, so that θ is a small additional phase shift due to the noise reduction circuitry. For a perfect differentiator, $\theta = 0$.

The output of the compensator of figure 5 is $e_\Sigma = e_1 - 2ke_2 + e_3$. Since θ is small, $\cos \theta \simeq 1$, $\sin \theta \simeq \theta$, and

$$e_\Sigma \simeq \mathscr{A} \left(1 - \frac{\omega_n^2}{\omega^2} \right) \sin \omega t + 2k \frac{\omega}{\omega_n} \cos \omega t$$

$$+ 2k\theta \frac{\omega}{\omega_n} \mathscr{A} \sin \omega t + 2\theta \mathscr{A} \frac{\omega^2}{\omega_n^2} \cos \omega t \tag{6}$$

Without the noise reduction modifications on the differentiators, the last two terms in equation (6) are not present, since $\theta = 0$. At $f = f_n$, the first term vanishes, and if $k = \zeta$, the damping coefficient of the anemometer, $e_\Sigma = 2\zeta \mathscr{A} \cos \omega_n t$. This is what the compensator output should be for an input $\mathscr{A} \sin \omega_n t$.

Now consider the last two terms in equation (6), the error terms. Ordinarily $k \simeq \zeta$, which is small. The phase error θ is also small, so that the first error term, which contains the product $\theta\zeta$, can be ignored. It is the second error term which predominates. For $\omega \simeq \omega_n$, $e_\Sigma \simeq 2\mathscr{A}(k + \theta) \cos \omega t$. As long as $\zeta > \theta$, which occurs for moderately high damping, the value of k can be adjusted so that $k + \theta = \zeta$, and the compensator has the correct output $2\mathscr{A}\zeta \cos \omega_n t$ at f_n. For the compensator built at the Lewis Research Center, the value of θ at $\omega = \omega_n$ is about 0.1 while the typical drag force anemometer has a damping coefficient which does not exceed about

0.03. In this case $\zeta < \theta$ so k must be negative to have $k + \theta = \zeta$. This is accomplished merely by removing the inverter from the circuit of figure 5. The exact value for the minimum damping coefficient which can be accommodated without removing the inverter depends on the values of the extra resistor and capacitor added to the differentiator to reduce the gain at high frequencies and on the natural frequency of the anemometer. An exact formula is given in appendix B.

The above discussion indicates that it is only necessary to adjust the damping control, but the more elaborate analysis of appendix B shows that both the amplitude and phase must be considered and that the natural frequency control must also be adjusted slightly. Nevertheless, the basic idea is to use a small amount of the signal from the first differentiator to cancel the overall phase error which results from using the modified differentiators.

RESULTS

The results discussed in this section are both computed and experimental, and are based on the compensator circuit shown in figure 9. For the theoretical curves, the settings of the natural frequency and damping controls were determined as explained in the example in appendix B. A spectrum analyzer was used to obtain these settings for the experimental curves. The controls were adjusted by eye to give the smoothest curve on the spectrum analyzer in the region of the natural frequency while the beam was excited by flow from an open jet with turbulence frequency components extending beyond f_n.

The first of the computed results (fig. 10) can be compared to figure 8 to see the results of removing the inverter. The improvement in suppressing the large increase in gain for frequencies near f_n is apparent.

The next two figures (figs. 11 and 12) are the computed and experimental results for a drag force anemometer with $f_n = 1300$ Hz and $\zeta = 0.024$. To obtain figure 12, the beam was excited by the turbulence in the flow in a half-inch diameter free jet.

The calculated frequency response for a high frequency anemometer is shown in figure 13. It has a natural frequency of 42.8 kHz and damping coefficient of 0.007. The transient response of this anemometer was also measured by placing it in front of a shock tube, as shown in figure 14. Figure 15 shows the output of this anemometer with no compensator in the circuit. The characteristic ringing is quite evident. The next figure (fig. 16) shows the results when the compensator is added to the circuit. The ringing is suppressed and the shock profile can be seen much more clearly.

The last figure is the shock profile measured with an infinite line pressure probe, which has no characteristic natural frequency, and frequency response which is estimated to be flat out to the 50 to 100 kHz region.

CONCLUDING REMARKS

This paper has discussed the electronic frequency compensation of second order systems, particularly those such as the drag force anemometer which have small damping coefficients.

The electronic frequency compensator has two differentiators which must be modified to reduce their high frequency gain. It was shown in this report that because of these modifications, lightly damped systems are not as adequately compensated near their natural frequencies as they might be.

A simple circuit modification, that of removing the inverter from the conventional circuit, was shown to improve the compensation near f_n. Numerical calculations, consisting of computer generated frequency response curves, and some experimental frequency response and some transient response curves were presented showing that adequate compensation can be achieved in practice.

APPENDIX A

$\mathscr{A}$	amplitude
A,B	undetermined coefficients of solution of differential equation
C_1	input capacitor
C_f	feedback capacitor
e_1	compensator input
e_Σ	compensator ouput
e_2	ouput of first differentiator
e_3	ouput of second differentiator
$\mathscr{E}_o$	κP_o
f	frequency, Hz
F	force, newtons
k	setting of damping adjustment
n	(subscript) natural
P_o	pressure amplitude
R	resultant coefficient of solution of differential equation
R_1	input resistor
R_f	feedback resistor
t	time
T_1, T_2	partial amplitude of compensator signal
x	output of drag force anemometer
Δ	determinant
ζ	damping coefficient
θ_1	$\tan^{-1} \omega/\omega_1$
θ_f	$\tan^{-1} \omega/\omega_f$
θ	$\theta_1 + \theta_f$
κ	proportionality constant
φ	phase shift due to anemometer
φ_Σ	phase shift due to compensator
ω_1	$(R_1C_1)^{-1}$
ω_f	$(R_fC_f)^{-1}$
ω_c	$(R_fC_1)^{-1}$

APPENDIX B

It is shown in this appendix that it is possible to achieve acceptable amplitude compensation of second order system even while using differentiators modified to reduce their gain at high frequencies, so that circuit stability is increased and noise is reduced. What shall be done is to assume an input into the sensor which is to be compensated, and then examine the overall response of the sensor and compensator.

It is convenient to take the input to be of the form $P_o \sin \omega t$. In the case of the drag force anemometer, P_o is the amplitude of the variation in velocity head. The output $x(t)$ of the anemometer is related to the input by the differential equation

$$\frac{\ddot{x}}{\omega_n^2} + \frac{2\zeta}{\omega_n}\dot{x} + x = \kappa P_o \sin \omega t = \mathscr{E}_o \sin \omega t \qquad \text{(B1)}$$

The two parameters which characterize the second order system are the natural frequency $f_n = \omega_n/2\pi$ and the damping coefficient ζ. Equation (B1) has solution

$$x(t) = A \sin \omega t + B \cos \omega t = \sqrt{A^2 + B^2} \sin (\omega t_o - \varphi), \quad \varphi = -\tan^{-1} \frac{B}{A} \qquad \text{(B2)}$$

$$\left.\begin{aligned} A &= \mathscr{E}_o \left(1 - \frac{\omega^2}{\omega_n^2}\right) \Big/ \Delta \\ B &= -2z\, \mathscr{E}_o \frac{\omega}{\omega_n} \Big/ \Delta \\ \Delta &= \left(1 - \frac{\omega^2}{\omega_n^2}\right)^2 + 4\zeta^2 \frac{\omega^2}{\omega_n^2} \end{aligned}\right\} \qquad \text{(B3)}$$

In terms of amplitude and phase,

$$\left.\begin{aligned} \sqrt{A^2 + B^2} &= \mathscr{E}_o \Big/ \sqrt{\left(1 - \frac{\omega^2}{\omega_n^2}\right)^2 + 4\zeta^2 \frac{\omega^2}{\omega_n^2}} \\ \tan \varphi &= \frac{2\zeta \frac{\omega}{\omega_n}}{\left(1 - \frac{\omega^2}{\omega_n^2}\right)} \end{aligned}\right\} \qquad \text{(B4)}$$

In order to reduce the noise associated with the differentiators, they are modified as shown in figure 6. If e_1 is the input to the modified differentiator, and e_2 is the output, it is shown in reference 3 that e_1 and e_2 are related by

$$e_2 = \frac{-\frac{P}{\omega_c}}{\left(1 + \frac{P}{\omega_1}\right)\left(1 + \frac{P}{\omega_f}\right)} e_1 \tag{B5}$$

In equation (B5), P stands for $\frac{d}{dt}$, ω_1 for $\frac{1}{R_1 C_1}$, ω_f for $\frac{1}{R_f C_f}$, and ω_c for $\frac{1}{R_f C_1}$. In our case, e_1, which is the input to the first differentiator, is the output from the drag force anemometer, $x(t) = A \sin \omega t + B \cos \omega t$. Then (B5) yields a differential equation for e_2, which is

$$\left[1 + \left(\frac{1}{\omega_1} + \frac{1}{\omega_f}\right)\frac{d}{dt} + \frac{1}{\omega_1 \omega_f}\frac{d^2}{dt^2}\right] e_2 = -\frac{\omega}{\omega_c}\frac{d}{dt}[A \sin \omega t + B \cos \omega t]$$

$$= -\frac{\omega}{\omega_c}[A \cos \omega t - B \sin \omega t] \tag{B6}$$

Equation (B6) is solved by letting $e_2 = C \sin \omega t + D \cos \omega t$ and then solving for C and D, which satisfy the algebraic equations

$$\left.\begin{aligned} C\left[1 - \left(\frac{\omega^2}{\omega_1 \omega_f}\right)\right] - D\left(\frac{\omega}{\omega_1} + \frac{\omega}{\omega_f}\right) &= B\frac{\omega}{\omega_c} \\ C\left(\frac{\omega}{\omega_1} + \frac{\omega}{\omega_f}\right) + D\left[1 - \frac{\omega^2}{\omega_1 \omega_f}\right] &= -A\frac{\omega}{\omega_c} \end{aligned}\right\} \tag{B7}$$

Using this solution,

$$e_2 = -\frac{\omega/\omega_c}{\left(1 + \frac{\omega^2}{\omega_1^2}\right)\left(1 + \frac{\omega^2}{\omega_f^2}\right)} \left\{\left[A\left(\frac{\omega}{\omega_1} + \frac{\omega}{\omega_f}\right) - B\left(1 - \frac{\omega^2}{\omega_1 \omega_f}\right)\right] \sin \omega t \right.$$

$$\left. + \left[A\left(1 - \frac{\omega^2}{\omega_1 \omega_f}\right) + B\left(\frac{\omega}{\omega_1} + \frac{\omega}{\omega_f}\right)\right] \cos \omega t \right\} \tag{B8}$$

This may be more compactly written as

$$e_2 = -\sqrt{A^2 + B^2}\ \frac{\omega/\omega_c}{\sqrt{1 + \frac{\omega^2}{\omega_1^2}}\sqrt{1 + \frac{\omega^2}{\omega_f^2}}} \cos(\omega t - \theta'), \tag{B9}$$

$$\tan\theta' = \tan[(\theta_1 + \theta_f) + \varphi] \equiv \tan(\theta + \varphi)$$

In equation (B9),

$$\tan\theta_1 \equiv \frac{\omega}{\omega_1}\ ,\ \tan\theta_f \equiv \frac{\omega}{\omega_f}\ ,\ \theta \equiv \theta_1 + \theta_f$$

The phase shift φ due to the drag force anemometer is $-\tan^{-1} B/A$ as in equation (B4).

With these definitions,

$$\cos\theta_1 = \frac{1}{\sqrt{1 + \omega^2/\omega_1^2}}\ ,\ \cos\theta_f = \frac{1}{\sqrt{1 + \omega^2/\omega_f^2}}$$

$$e_2 = -\sqrt{A^2 + B^2}\ \frac{\omega}{\omega_c} \cos\theta_1 \cos\theta_f \cos[(\omega t - \varphi) - \theta]$$

$$= \sqrt{A^2 + B^2}\ \frac{\omega}{\omega_c} \cos\theta_1 \cos\theta_f \sin[(\omega t - \varphi) - (\tfrac{\pi}{2} + \theta)] \tag{B10}$$

The output of the first differentiator, e_2, is the input of the second, whose output is called e_3. Using (B10), e_3 is easily written down; it is

$$e_3 = \sqrt{A^2 + B^2}\ \frac{\omega^2}{\omega_c^2} \cos^2\theta_1 \cos^2\theta_f \sin[(\omega t - \varphi) - 2(\tfrac{\pi}{2} + \theta)]$$

$$= -\sqrt{A^2 + B^2}\ \frac{\omega^2}{\omega_c^2} \cos^2\theta_1 \cos^2\theta_f \sin[(\omega t - \varphi) - 2\theta] \tag{B11}$$

The output of the compensator is called e_Σ. As shown in figure 5, if the inverter has been removed and k is the setting of the damping adjustment

$$e_\Sigma = e_1 + 2\,k\,e_2 + e_3$$

$$= \sqrt{A^2 + B^2}\left\{\sin(\omega t + \varphi) - 2\,k\,\frac{\omega}{\omega_c}\cos\theta_1\cos\theta_f\cos[(\omega t - \varphi) - \theta]\right.$$

$$\left. - \frac{\omega^2}{\omega_c^2}\cos^2\theta_1\cos^2\theta_f\sin[(\omega t - \varphi) - 2\theta]\right.$$

$$\left. = \sqrt{A^2 + B^2}\,[T_1\sin(\omega t - \varphi) + T_2\cos(\omega t - \varphi)]\right\} \qquad \text{(B12)}$$

where

$$\left.\begin{aligned} T_1 &= 1 - 2\,k\,\frac{\omega}{\omega_c}\cos\theta_1\cos\theta_f\sin\theta - \frac{\omega^2}{\omega_c^2}\cos^2\theta_1\cos^2\theta_f\cos 2\theta \\ T_2 &= -2\,k\,\frac{\omega}{\omega_c}\cos\theta_1\cos_f\cos\theta + \frac{\omega^2}{\omega_c^2}\cos^2\theta_1\cos^2\theta_f\sin 2\theta \end{aligned}\right\} \qquad \text{(B13)}$$

Using the identities $\sqrt{A^2 + B^2}\sin(\omega t - \varphi) = A\sin\omega t + B\cos\omega t$ and $\sqrt{A^2 + B^2}\cos(\omega t - \varphi) = A\cos\omega t - B\sin\omega t$, equation (B12) can be written

$$e_\Sigma = (AT_1 - BT_2)\sin\omega t + (BT_1 + AT_2)\cos\omega t$$

$$= \sqrt{A^2 + B^2}\sqrt{T_1^2 + T_2^2}\sin(\omega t + \varphi_T)$$

where

$$\tan \varphi_T = \frac{BT_1 + AT_2}{AT_1 - BT_2} = \frac{\dfrac{B}{A} + \dfrac{T_2}{T_1}}{1 - \dfrac{B}{A}\dfrac{T_2}{T_1}} = \frac{-\tan \varphi + \tan \varphi_\Sigma}{1 + \tan \varphi \tan \varphi_\Sigma} = \tan (\varphi_\Sigma - \varphi) \qquad \text{(B14)}$$

The amplitude is the product of the amplitudes due to the sensor $\left(\sqrt{A^2 + B^2}\right)$ and the compensator $\left(\sqrt{T_1^2 + T_2^2}\right)$ and the total phase shift φ_T is the sum of the two phase shifts, φ due to the sensor and φ_Σ due to the compensator.

Now the purpose of the compensator is to undo the effect of the probe so that the output of the compensator is equal to the input to the anemometer; that is, $e_\Sigma = \mathscr{E}_0 \sin \omega t$ for all ω. Unfortunately, perfect compensation with this circuit is not possible for all ω. Choosing the match at $\omega = \omega_n$, however, turns out to be a good choice, since it results in excellent amplitude compensation to well beyond ω_n. At $\omega = \omega_n$, then, equation (B14) gives

$$(AT_1 - BT_2)\Big|_{\omega_n} = \mathscr{E}_0 \qquad (BT_1 + AT_2)\Big|_{\omega_n} = 0 \qquad \text{(B15)}$$

At $\omega = \omega_n$, $A = 0$ and $B = -\mathscr{E}_0/2\zeta$, so equations (B13) and (B15) give

$$\left.\begin{aligned} 1 - 2k \frac{\omega_n}{\omega_c} \cos \theta_{1n} \cos \theta_{fn} \sin \theta_n - \frac{\omega_n^2}{\omega_c^2} \cos^2 \theta_{1n} \cos^2 \theta_{fn} \cos 2\theta_n = 0 \\ -2k \frac{\omega_n}{\omega_c} \cos \theta_{1n} \cos \theta_{fn} \cos \theta_n + \frac{\omega_n^2}{\omega_c^2} \cos^2 \theta_{1n} \cos^2 \theta_{fn} \sin 2\theta_n = 2\zeta \end{aligned}\right\} \text{(B16)}$$

The subscript n means that the quantity is evaluated at the natural frequency.

The solution of (B16) for ω_n/ω_c and $2k$ is

$$\left.\begin{aligned} \frac{\omega_n}{\omega_c} &= \sqrt{\frac{1 + 2\,\zeta\,\tan\theta_n}{\cos\theta_{1n}\cos\theta_{fn}}} \\ 2\,k &= \frac{\sin 2\,\theta_n - 2\,\zeta\cos 2\,\theta_n}{\cos\theta_n\sqrt{1 + 2\,\zeta\,\tan\theta_n}} \end{aligned}\right\} \qquad \text{(B17)}$$

These are the settings required for the natural frequency and damping coefficient controls to give exact compensation at $\omega = \omega_n$. Note that if perfect differentiators had been used, the equations (B17) reduce to $\omega_n/\omega_c = 1$ and $2\,k = -2\,\zeta$, since then $\theta_n = 0$. The result $\omega_n/\omega_c = 1$ means that the natural frequency control is set at f_n, and the result $2\,k = -2\,\zeta$ means that the damping coefficient control is set at ζ. The minus sign means that the inverter is in the circuit.

The second of equations (B17) provides a means of distinguishing between "high" and "low" damping. If the numerator is positive ($\zeta < 1/2 \tan 2\,\theta_n$), the inverter is not in the circuit and this is the low damping case. On the other hand, if the numerator is negative ($\zeta > 1/2 \tan 2\,\theta_n$), the inverter is required and this is the high damping case.

The value of ζ which establishes the boundary between the high and low damping cases depends on the values of the extra resistor and capacitor added to the differentiator circuits to reduce high frequency noise and on the natural frequency of the anemometer. This value of ζ is about 0.105 for $f_n = 1300$ and is about 0.18 for $f_n = 42.8$ kHz for the circuit shown in figure 9.

The compensator schematic is shown in figure 9. It has $R_1 = 505\ \Omega$, $C_1 = 510$ pF and $C_f = 51$ pF. These values were chosen in accord with acceptable practice (ref. 5). The value of R_f varies from 0 to 50 kΩ to give the desired value for ω_c. (Fixed 250 kΩ resistors were added to allow for an f_n of 1300 Hz.)

Since the formula in (B17) for ω_n/ω_c implicitly involves ω_n/ω_c on the right side also, for example, through

$$\cos\theta_{fn} = \left(1 + \frac{\omega_n^2}{\omega_f^2}\right)^{1/2} = \left[1 + \left(\frac{\omega_n}{\omega_c}\frac{\omega_c}{\omega_f}\right)^2\right]^{1/2}$$

it is still necessary to solve for ω_n/ω_c. This can be done algebraically but the result is a complicated cubic equation, so it is easier to solve by iteration. The form

$$\frac{\omega_n}{\omega_c} = \left\{\left[1 + 2\,z\,\tan\left(\tan^{-1}\frac{\omega_n}{\omega_1} + \tan^{-1}\left[\frac{\omega_n}{\omega_c}\,\frac{\omega_c}{\omega_f}\right]\right)\right]\left[1 + \frac{n\omega^2}{\omega_1^2}\right]\left[1 + \left(\frac{c\omega}{\omega_f}\frac{n\omega}{\omega_c}\right)^2\right]\right\}^{1/2} \qquad \text{(B18)}$$

converges to ten places after about six iterations, starting with $\omega_n/\omega_c = 1$. For the example under consideration, $\omega_n/\omega_1 = 2\pi f_n R_1 C_1 = (2\pi \times 1300) \times (505 \times 510 \times 10^{-12}) = 2.104 \times 10^{-3}$ and $\omega_c/\omega_f = R_f C_f / R_f C_1 = C_f/C_1 = 0.1$. For this case, $\omega_n/\omega_c = 1.008$. Once ω_n/ω_c has been found, 2 k is determined from the second of equations (B17). For this example, 2 k = 0.1568. Having found ω_n/ω_c and 2 k, T_1 and T_2 are obtained from (B13). This is sufficient to calculate the overall response, as is done in figure 10.

REFERENCES

1. Shepard, C. E.; and Warshawsky, I.: Electrical Techniques for Time Lag Compensation of Thermocouples used in Jet Engine Gas Temperature Measurements. ISA Pro., 1952, pp. 149-154.
2. Krause, Lloyd N.; and Fralick, Gustave C.: Miniature Drag-Force Anemometer. NASA TM X-3507.
3. Schweppe, J. L.; et al.: Methods for the Dynamic Calibration of Pressure Transducers. NBS Monograph 67, National Bureau of Standards., 1963.
4. Jackson, Albert S.: Analog Computation, McGraw-Hill Book Co. 1960, p. 146.
5. Philbrick/Nexus Research Co.: Applications Manual for Operational Amplifiers. Second ed. Philbrick/Nexus Research, 1968, p. II. 21.

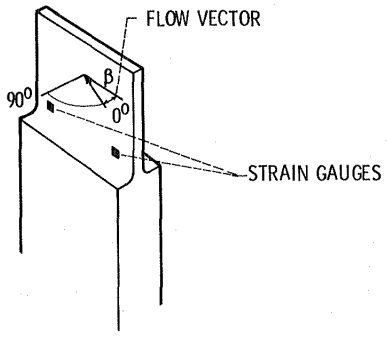

Figure 1. - Drag force anemometer showing flow direction relative to beam: $\beta \approx 0$: output proportional to product of velocity head and β. $\beta \approx 90^0$: output proportional to velocity head.

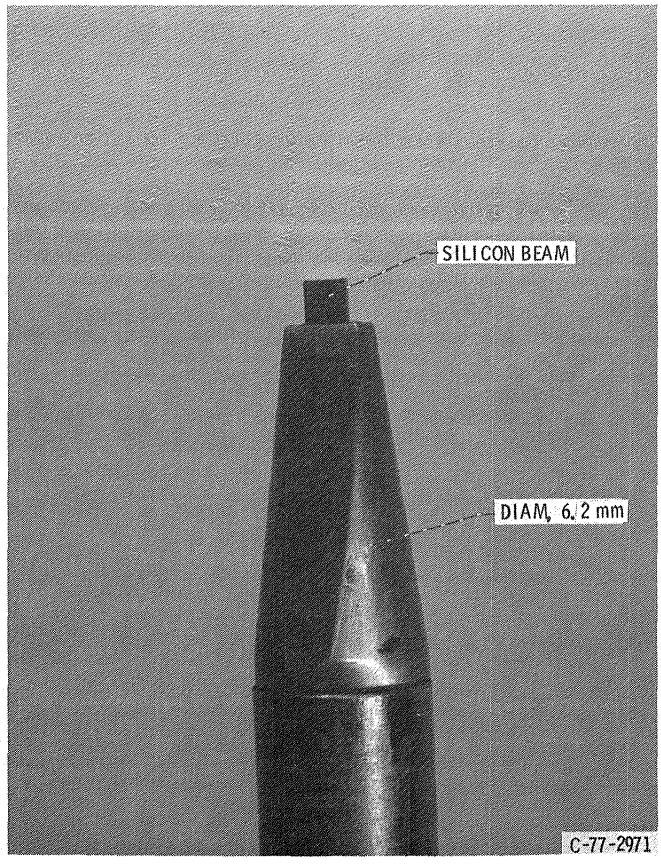

Figure 2. - Drag-force anemometer.

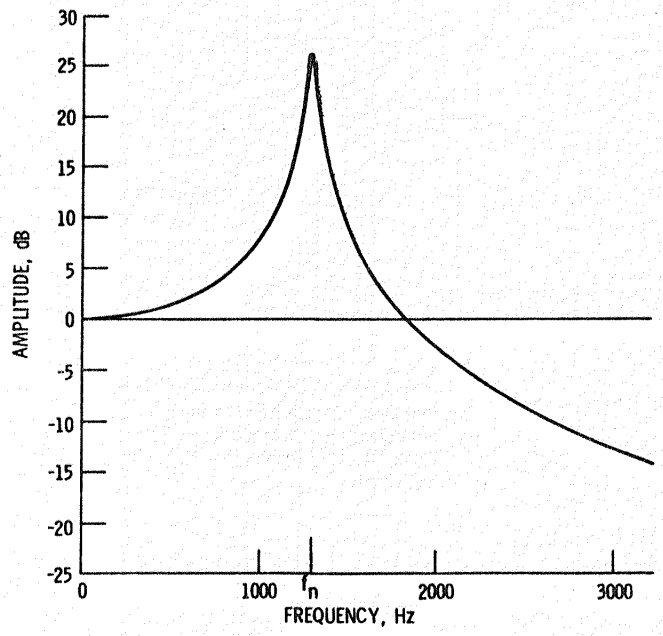

Figure 3. - Frequency response of second order system natural frequency = 1300 Hz, damping coefficient = 0.024.

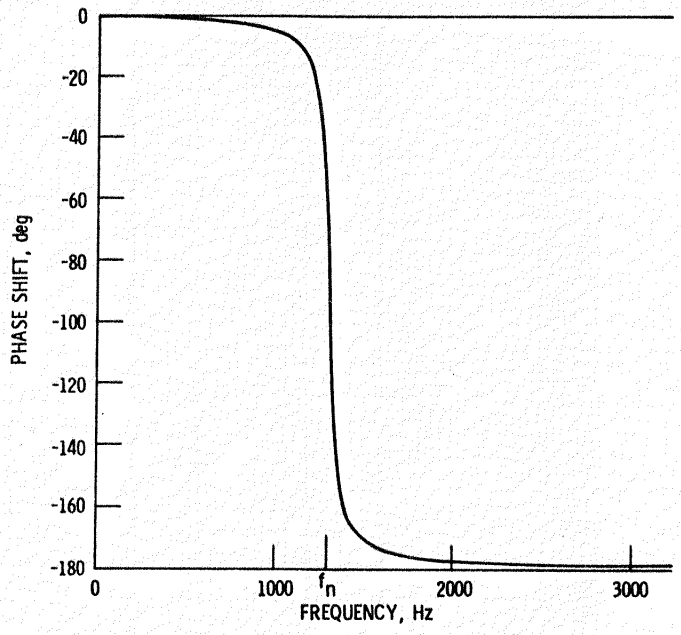

Figure 4. - Output phase shift of second order system natural frequency = 1300 Hz, damping coefficient = 0.024.

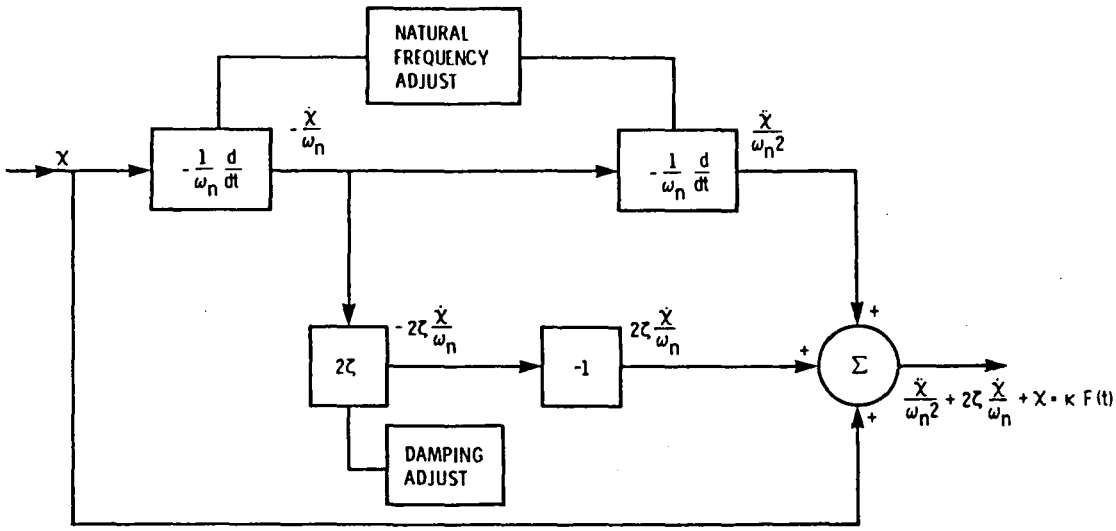

Figure 5. - Block diagram of compensator.

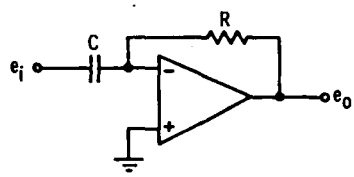

$$e_o = -RC\frac{de_i}{dt}$$

(a)

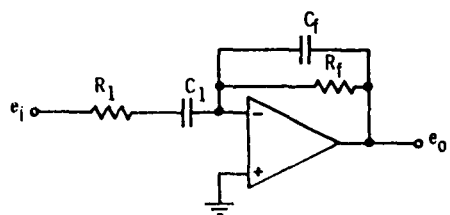

$$e_o = -R_f C_1 \frac{de_i}{dt} - \left[R_1 C_1 R_f C_f \frac{d^2 e_o}{dt^2} + (R_1 C_1 + R_f C_f)\frac{de_o}{dt}\right]$$

(b)

(a) Pure differentiator.

(b) Modified differentiator.

Figure 6. - Ordinary differentiator circuit and differentiator circuit modified for reduced noise.

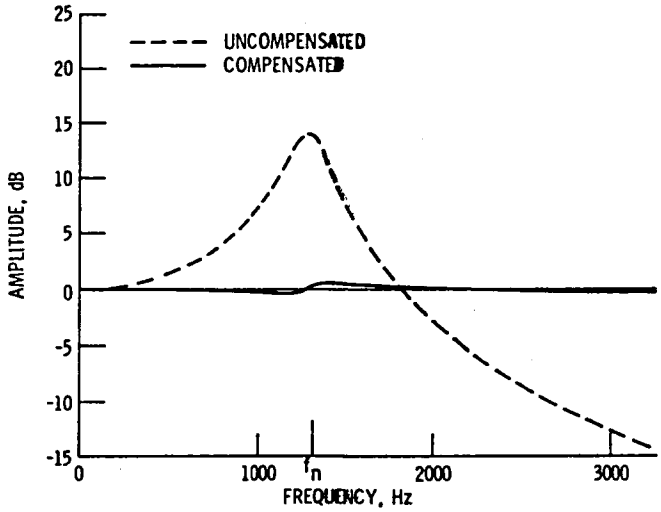

Figure 7. - Calculated output frequency response for uncompensated and conventially compensated second order system (natural frequency = 1300 Hz, damping coefficient = 0.1) compensator controls set for zero output at peak of second order system.

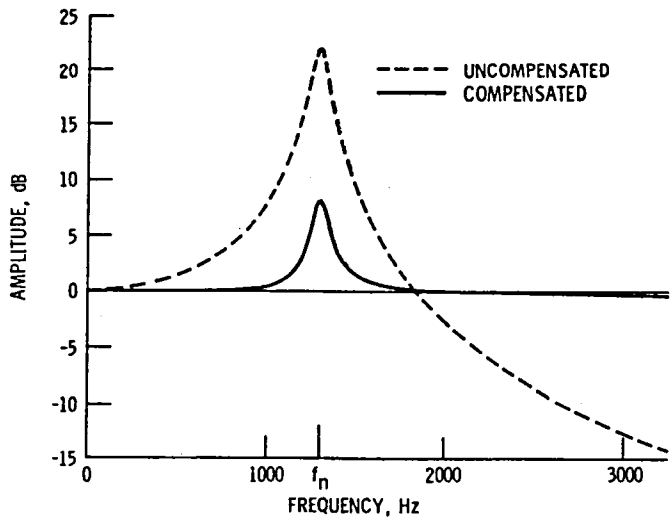

Figure 8. - Calculated output frequency response for uncompensated and conventionally compensated second order system (natural frequency = 1300 Hz, damping coefficient = 0.04) compensator controls set for minimum output at peak of second order system.

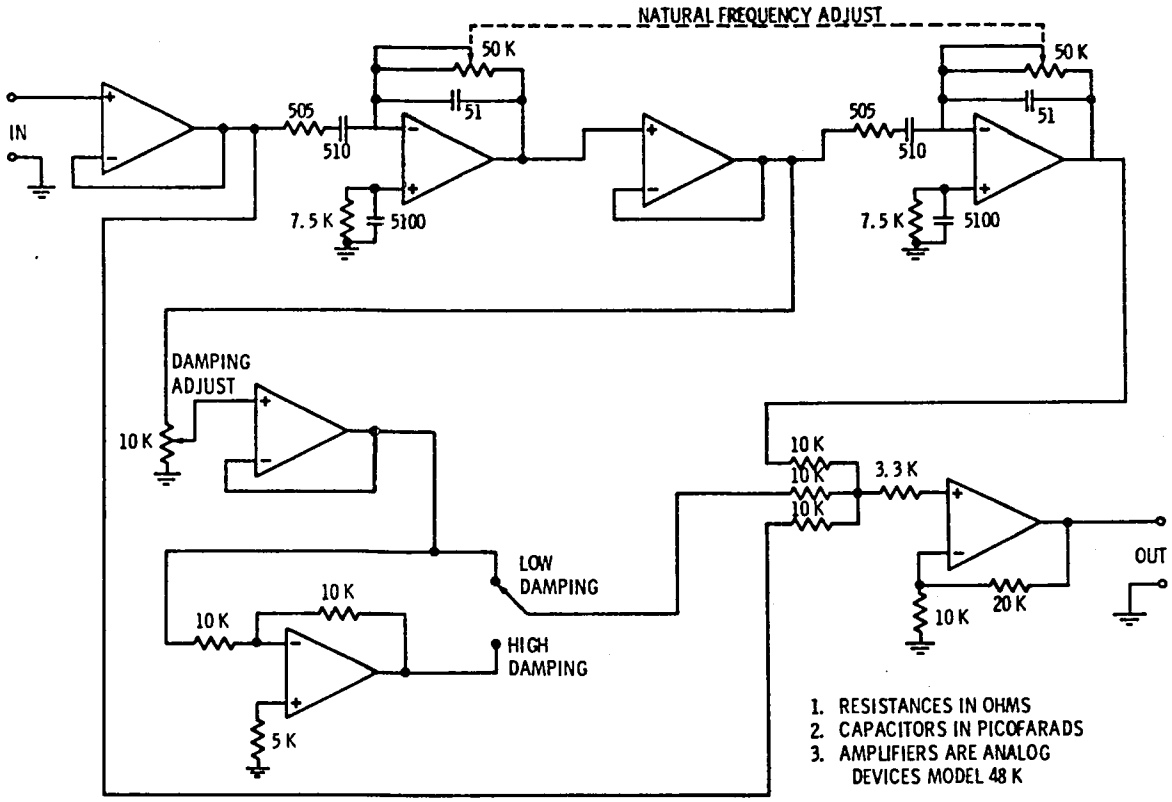

Figure 9. - Compensator circuit.

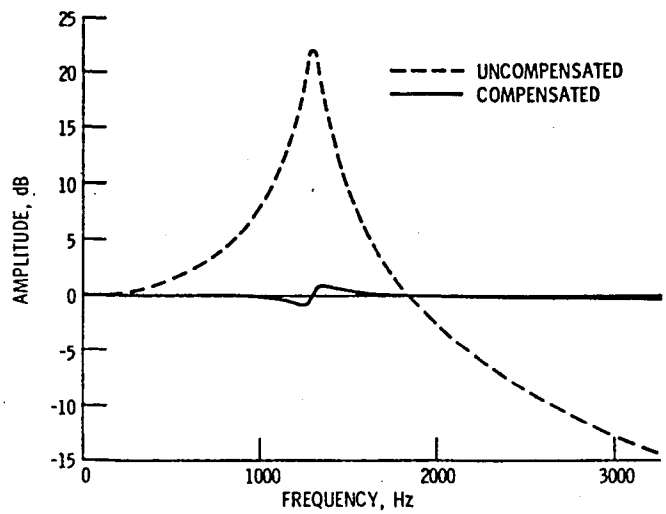

Figure 10. - Calculated output frequency response for uncompensated and compensated (with modified design compensator) second order system (natural frequency = 1300 Hz, damping coefficient = 0.04) compensator controls set for zero output at peak of second order system.

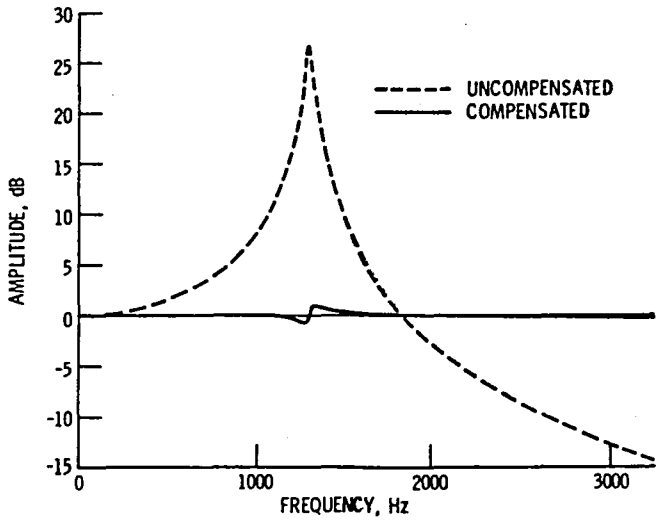

Figure 11. - Computed output frequency response for compensated (with modified design compensator) and uncompensated second order system (natural frequency = 1300 Hz, damping coefficient = 0.024) compensator controls set for zero output at peak of second order system.

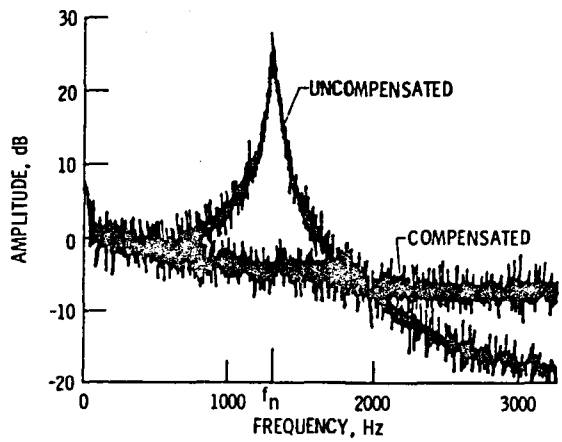

Figure 12. - Measured frequency response for compensated (with modified design compensator) and uncompensated second order system (natural frequency = 1300 Hz, damping coefficient = 0.024) compensator controls set for zero output at peak of second order system.

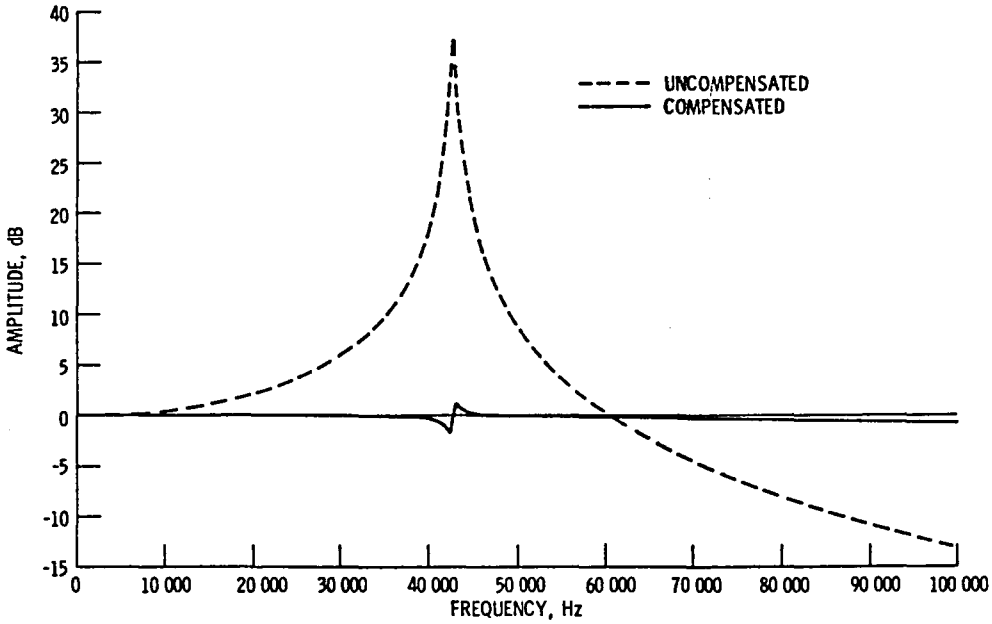

Figure 13. - Computed output frequency response for compensated (with modified design compensator) and uncompensated second order system (natural frequency = 42.8 kHz, damping coefficient = 0.007) compensator controls set for zero output at peak of second order system.

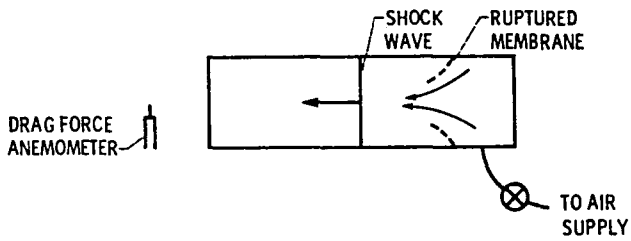

Figure 14. - Location of drag force anemometer in front of shock tube.

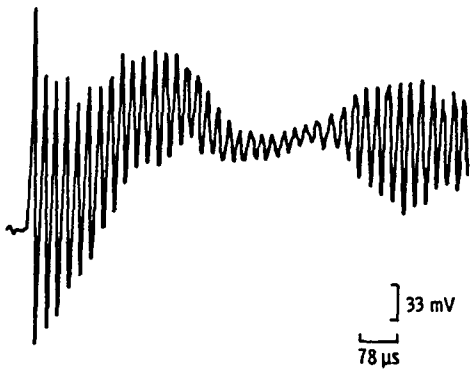

Figure 15. - Transient response of uncompensated drag force anemometer to shock wave.

Figure 16. - Transient response of compensated (with modified design compensator) to shock wave.

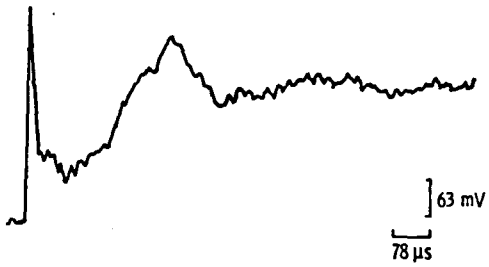

Figure 17. - Transient response of infinite line pressure probe to shock wave.

1. Report No. NASA TM-82927	2. Government Accession No.	3. Recipient's Catalog No.
4. Title and Subtitle EXTENDING THE FREQUENCY OF RESPONSE OF LIGHTLY DAMPED SECOND ORDER SYSTEMS: APPLICATION TO THE DRAG FORCE ANEMOMETER		5. Report Date August 1982 6. Performing Organization Code 505-32-82
7. Author(s) Gustave C. Fralick		8. Performing Organization Report No. E-1178 10. Work Unit No.
9. Performing Organization Name and Address National Aeronautics and Space Administration Lewis Research Center Cleveland, Ohio 44135		11. Contract or Grant No. 13. Type of Report and Period Covered Technical Memorandum
12. Sponsoring Agency Name and Address National Aeronautics and Space Administration Washington, D. C. 20546		14. Sponsoring Agency Code
15. Supplementary Notes		

16. Abstract

It is shown in this paper that a conventional electronic frequency compensator does not provide adequate compensation near the resonant frequency of a lightly damped second order system, such as the drag force anemometer. The reason for this is discussed, and a simple circuit modification is presented which overcomes the difficulty. The improvement is shown in theoretical frequency response curves as well as in the experimental results from some typical drag force anemometers.

17. Key Words (Suggested by Author(s))	18. Distribution Statement
Instrument compensation Frequency compensation Second order systems Anemometers	Unclassified - unlimited STAR Category 35

19. Security Classif. (of this report)	20. Security Classif. (of this page)	21. No. of Pages	22. Price*
Unclassified	Unclassified		

* For sale by the National Technical Information Service, Springfield, Virginia 22161

End of Document